

1-D Controlled source electromagnetic forward modeling for marine gas hydrates studies*

Zhao Luanxiao¹, Geng Jianhua¹, Zhang Shengye², and Yang Dikun²

Abstract: We discuss the feasibility of using controlled-source electromagnetic (CSEM) in the frequency domain for prospecting marine gas hydrates. Based on the Ocean Drilling Program (ODP) Leg 164 log data, we have established several 1-D resistivity models which have different gas hydrate concentrations. Meanwhile, we analyzed the electromagnetic response of marine gas hydrates in the frequency domain based on these models. We also studied the relationship between electrical field magnitude or phase and parameters such as receiver-transmitter distance and frequency. Our numerical modeling results provide us with a quantitative reference for exploration and resource evaluation of marine gas hydrates.

Keywords: gas hydrate, CSEM, forward modeling, resource evaluation

Introduction

Gas hydrates are ice-like white solids composed of natural gases and water which occur under appropriate conditions of high pressure and low temperature. They are a potential energy source for the 21st century and are getting more study. The lower boundary of the gas hydrate zone is generally identified on seismic sections by the bottom simulating reflector (BSR). However, the upper boundary of the hydrate bearing sediment is not clearly defined on reflection seismic sections. The total volume of hydrate and its resource value can not be evaluated accurately from seismic data alone. Gas hydrate, like ice, is an insulating material, so it naturally has a large contrast of physical properties for using EM methods for detection (Song et al., 2002; Ma et al., 2000; Song et al., 2001; Song et al., 2003).

Previously, many researchers have evaluated gas hydrates using marine EM methods (Yuan and Edwards, 2000; Edwards, 1997; Chave and Cox, 1982; Constable and Weiss, 2006), most of them only using transient

fields and only a few discussions were related to the electromagnetic response of marine gas hydrates with varying reservoir properties and detection device parameters in the frequency domain.

In this paper, the controlled source electromagnetic method uses an electric dipole as the electric-field source and several 1-D resistivity models with different gas hydrate concentration were established using ODP log data. Modeling results indicate that the calculated E-field magnitude and phase vary with parameters such as receiver-transmitter distance, frequency, and thickness. The calculated results provide reference information for the quantitative analysis of prospecting marine gas hydrates.

Method principles

The instrument configuration of the marine controlled-source electromagnetic method is different than the onshore configuration in that the discrete frequency

Manuscript received by the Editor November 11, 2007; revised manuscript received 18 March, 2008.

*This research is supported by the Program for New Century Excellent Talents in University (No. NCET-04-0370).

1) School of Ocean and Earth Science, Tongji University, Shanghai 200092, China

2) Institute of Geoscience and Geomatics, China University of Geoscience (Wuhan), Wuhan 430074, China

1-D Controlled source electromagnetic forward modeling

signals are transmitted by an electric dipole-dipole transmitter. The excited electromagnetic fields spread to the bottom and are measured by receivers located at different distances from the transmitting source. These receivers are linked in a linear array.

Assuming the vector direction of the electric dipole is along the x-axis, the E-field excited by the dipole source in the sea floor horizontal layers is expressed as (Tan et al., 2004):

$$E_x = -\frac{Ids}{4\pi} \int_0^\infty [(1-r_{TM}) \frac{u_0}{\hat{y}_0} - (1+r_{TE}) \frac{\hat{z}_0}{u_0}] \times [J_0(\lambda x) - \frac{1}{\lambda x} J_1(\lambda x)] dx - \frac{\hat{z}_0 Ids}{4\pi} \int_0^\infty (1+r_{TM}) \frac{\lambda}{u_0} J_0(\lambda x) dx, \quad (1)$$

$$r_{TM} = \frac{Z_0 - \hat{Z}_1}{Z_0 + \hat{Z}_1}, \quad (2)$$

$$r_{TE} = \frac{Y_0 - \hat{Y}_1}{Y_0 + \hat{Y}_1}. \quad (3)$$

If the sea floor is divided into N layers, then \hat{Y}_1 and \hat{Z}_1 can be calculated by the following recursive formulas:

$$\hat{Y}_1 = Y_1 \frac{\hat{Y}_2 + Y_1 \tanh(u_1 h_1)}{Y_1 + \hat{Y}_2 \tanh(u_1 h_1)}, \quad (4)$$

$$\hat{Y}_i = Y_i \frac{\hat{Y}_{i+1} + Y_i \tanh(u_i h_i)}{Y_i + \hat{Y}_{i+1} \tanh(u_i h_i)}, \quad (5)$$

$$\hat{Y}_N = Y_N, \quad (6)$$

$$\hat{Z}_1 = Z_1 \frac{\hat{Z}_2 + Z_1 \tanh(u_1 h_1)}{Z_1 + \hat{Z}_2 \tanh(u_1 h_1)}, \quad (7)$$

$$\hat{Z}_i = Z_i \frac{\hat{Z}_{i+1} + Z_i \tanh(u_i h_i)}{Z_i + \hat{Z}_{i+1} \tanh(u_i h_i)}, \quad (8)$$

$$\hat{Z}_N = Z_N. \quad (9)$$

Where

$$Y_i = \frac{u_i}{\hat{z}_i}, \quad (10)$$

$$Z_i = \frac{u_i}{\hat{y}_i}, \quad (11)$$

$$\hat{z}_i = i\mu_i w \approx i\mu_0 w, \quad (12)$$

$$\hat{y}_i = \sigma_i + i\varepsilon_i w, \quad (13)$$

$$u_i^2 = \lambda^2 + iw\mu_i \sigma_i. \quad (14)$$

These formulas, based on the digital filtering methods of the fast Hankel transform, are used to calculate the electric field amplitude and phase (Anderson, 1989; Constable and Weiss, 2006).

1-D-resistivity layer model building

The electrical conductivity of marine sediments is caused by the movement of particles in pore fluids. The empirical relationship between formation conductivity σ_f and porosity ϕ follows Archie's law:

$$\sigma_f = \phi^m S^n \sigma_w / A, \quad (15)$$

where m is the sediment cementation factor in the range of $1.5 < m < 3$, A is a constant in the range of $0.5 < A < 2.5$, S is the water saturation in the pores, n is the saturation exponent, and σ_w is the conductivity of the pore water. If we assume that A, m, and n are 2, then equation 15 can be rewritten as

$$\sigma_f = \phi^2 S_w^2 \sigma_w / 2. \quad (16)$$

We established the 1-D gas hydrate resistivity models based on the electric log data from Wells 994, 995, and 997 of the Ocean Drilling Program Leg 164 (Figure 1). Gas hydrate samples were taken from the drilled BSR zones in the Blake Ridge area off the east coast of North America during ODP Leg 164 and their average porosity is about 60% (Lu and McMechan, 2002; Hyndman et al., 1999). There are four models: M0 is the resistivity model with no gas hydrate in its marine sediments, while M1, M2, and M3 are models containing gas hydrate. We divided the gas hydrate bearing layer into four sub-layers, S1, S2, and S3 represent the hydrate saturation of the first, second, and third layers, respectively, while S4 is the gas saturation in the free gas layer (see Table 1). We suppose that the sediments with a thickness of 0 – 100 m overlying the hydrates have the same resistivity variation as the sea floor. The depth intervals of 100 – 170 m, 170 – 250 m, and 250 – 450 m are the first, second, and third layers and the 450 – 500 m interval is considered to be the free gas zone with lower resistivity. We consider 450 m to be the BSR depth.

Table 1 Gas hydrate saturation in each layer for modeling

| Model | S1 | S2 | S3 | S4 |
|-------|-----|-----|-----|----|
| M1 | 20% | 25% | 30% | 3% |
| M2 | 10% | 15% | 20% | 2% |
| M3 | 5% | 8% | 10% | 1% |

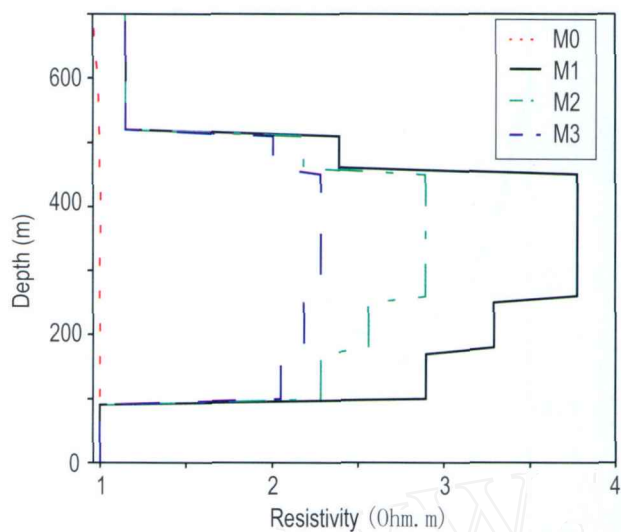


Fig. 1 1-D gas hydrate resistivity models.

Frequency domain electromagnetic response of marine gas hydrates

The variation of E-field magnitude with receiver-transmitter distance

We find that the E-field magnitude decreases with increasing receiver-transmitter distance in the four models and the gas hydrate model curves decay slower than the half-space model. As for the three gas hydrate models: M1, M2, and M3, the greater the gas hydrate concentration, the slower the decay of the E-field magnitude curve (Figure 2).

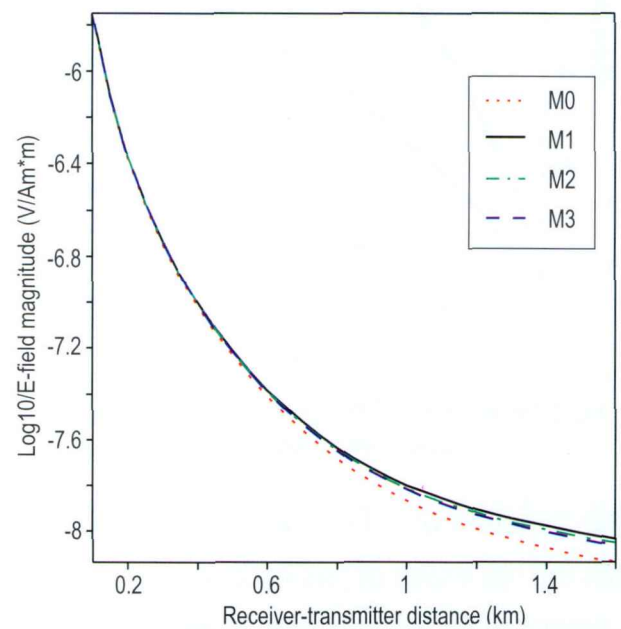


Fig.2 E-field curves versus receiver-transmitter distance for a frequency of 1 Hz.

The variation of E-field phase with receiver-transmitter distance

From Figure 3 we see that E-field phase in the four models increases with increasing receiver-transmitter distance at different frequencies, although the increase rate decreases at higher distances. The distinction between the model curves at a given frequency is not very clear. For a frequency of 1 Hz, the greater the concentrations of gas hydrate, the faster the E-field phase will increase with receiver-transmitter distance. For a frequency of 10 Hz, at shorter distances the greater the gas hydrate concentrations, the faster the E-field phase will increase with increasing receiver-transmitter distance. However, at larger receiver-transmitter distances, lower concentrations of gas hydrate, results in higher E-field phase will increase with increasing receiver-transmitter distance.

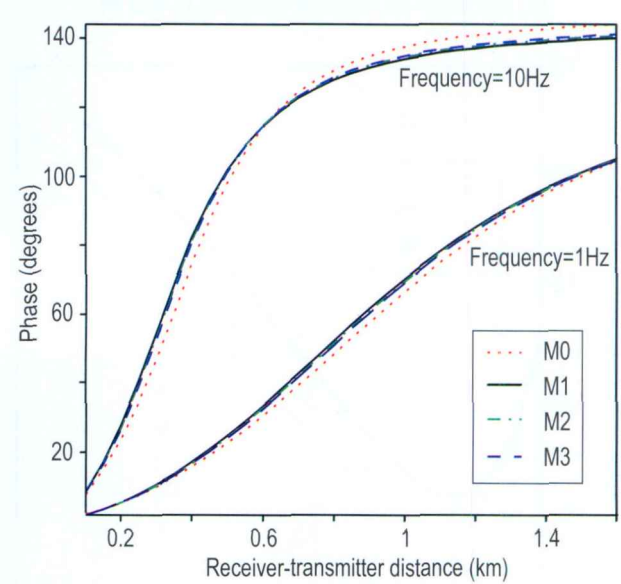
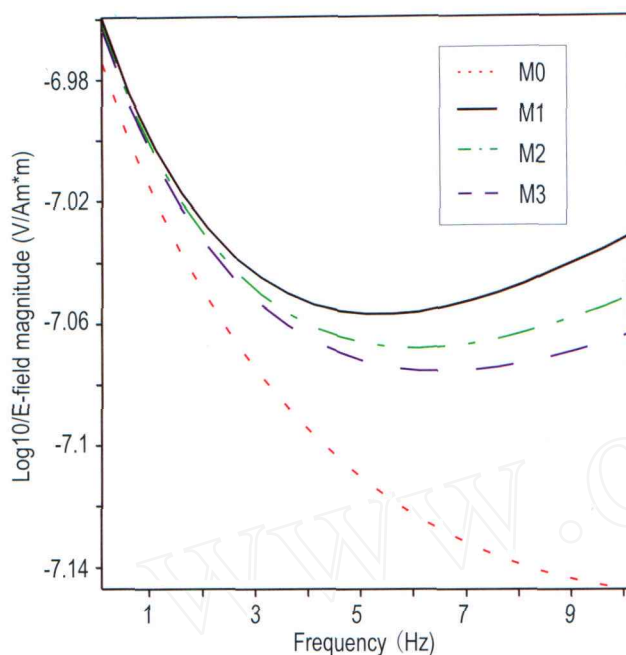


Fig. 3 E-field phase curves versus receiver-transmitter distance.

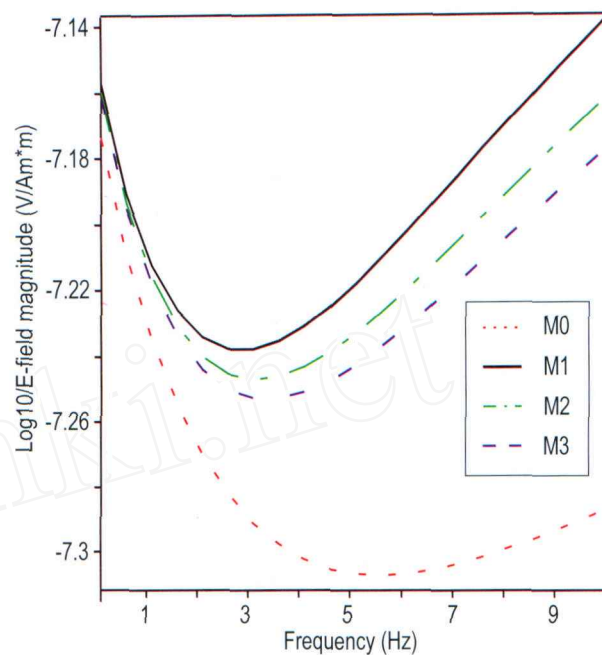
The variation of E-field magnitude with frequency

In Figure 4, we find that at low frequencies the E-field magnitude gradually decreases with increasing frequency. It reaches a minimum and then gradually increases with increasing frequency. For constant receiver-transmitter distance, greater gas hydrate concentrations result in slower E-field magnitude decrease with increasing frequency but after reaching the magnitude minimum, the increasing magnitude will increase relatively faster. Comparing the three panels in Figure 4, we see that for the same concentration of gas hydrate, at greater receiver-transmitter distances the minimum E-field magnitude is at lower frequencies.

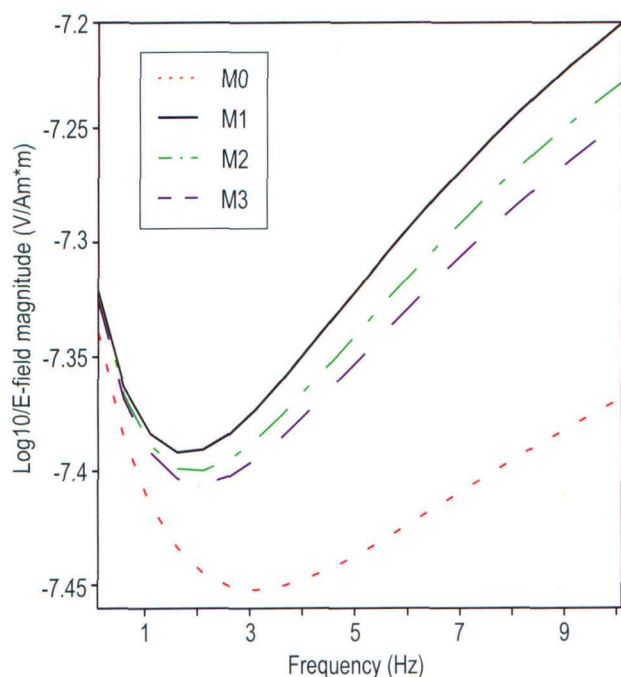
1-D Controlled source electromagnetic forward modeling



(a) Receiver-transmitter distance is 400 m.



(b) Receiver-transmitter distance is 500 m.



(c) Receiver-transmitter distance is 600 m.

Fig.4 E-field magnitude versus frequency at different receiver-transmitter distances.

distance and higher frequency, lower concentrations of the gas hydrate result in faster E-field phase increase. Comparing the three cases, we can also conclude that, at greater receiver-transmitter distance, the extent where E-field phase varies with frequency is greater.

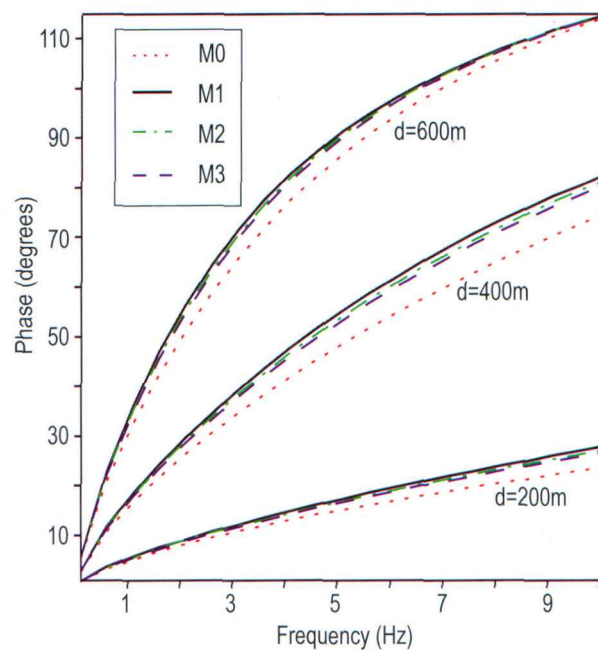


Fig. 5 The variation of E-field phase with frequency (d is the receiver-transmitter distance).

The variation of E-field phase with frequency

Figure 5 shows E-field phase versus frequency at three different receiver-transmitter distances. (1) E-field phase increases with increasing frequency and the amount of curve separation is greater than E-field phase versus receiver-transmitter distance.; (2) In the case of shorter receiver-transmitter distance, the greater the gas hydrate concentration, the faster the E-field phase will increase; (3) Under greater receiver-transmitter

The variation of E-field magnitude and phase with the thickness of gas hydrate

Figure 6 shows that E-field magnitude and phase show an approximate linear increase with the thickness of the reservoir. This relationship E-field magnitude and phase

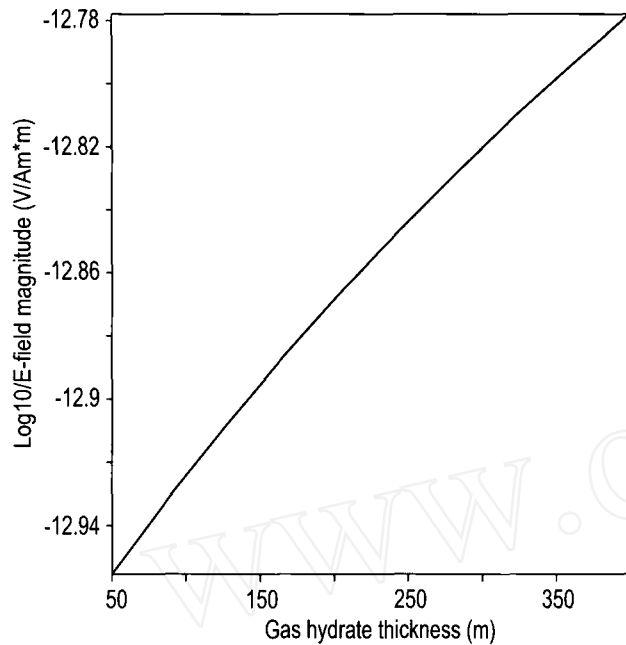


Fig. 6 (a) E-field magnitude versus gas hydrate thickness for model M1 with 1 Hz frequency and 1 km receiver-transmitter distance.

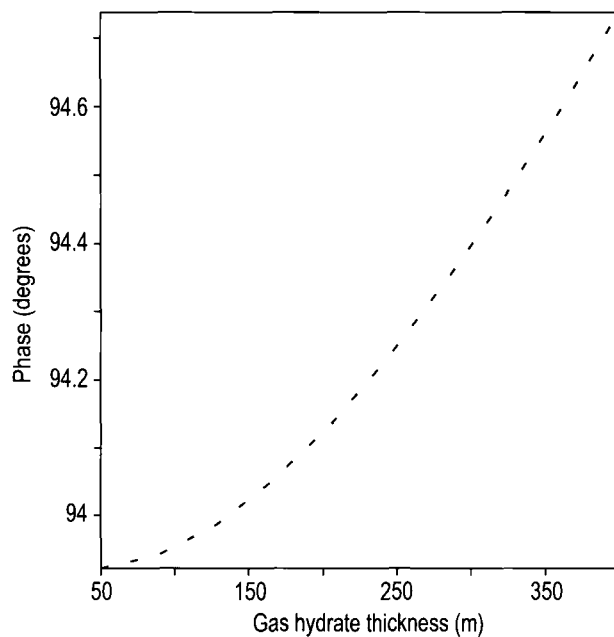


Fig.6 (b) The variation of E-field phase for model 1 with 1 Hz frequency and 1 km receiver-transmitter distance.

to gas hydrate thickness provides useful information for evaluating resource volume and thickness.

Conclusions

Through the 1-D forward modeling study of gas hydrates using the controlled source electromagnetic method, we computed features of the electromagnetic response of marine gas hydrates versus reservoir

parameters and acquisition parameters in the frequency domain. The results provide an important quantitative analysis reference for prospecting gas hydrates using CSEM methods.

The 1-D forward modeling study is insufficient to describe the actual distribution of gas hydrates, so 2-D and 3-D forward modeling studies will be needed in the future. In addition, the generation of gas hydrates is closely related to water pressure and temperature, so it will be necessary to use continuous anisotropic models and computations.

References

- Anderson, W. L., 1989, A hybrid fast Hankel transform algorithm for electromagnetic modeling: *Geophysics*, **54**, 263 – 266.
- Chave, A. D., and Cox, C. S., 1982, Controlled electromagnetic sources for measuring electrical conductivity beneath the oceans: forward problem and model study: *Journal of Geophysical Research*, **87**, 5327 – 5338.
- Constable, S., and Weiss, J. C., 2006, Mapping thin resistors and hydrocarbons with marine EM methods: insights from 1D modeling: *Geophysics*, **71**(2), G43 – G51.
- Edwards, R. N., 1997, On the resource evaluation of marine gas hydrate deposits using sea-floor transient electric dipole-dipole methods: *Geophysics*, **62**, 63 – 74.
- Edwards, N., 2005, Marine controlled source electromagnetics: principles, methodologies, future commercial applications: *Surveys in Geophysics*, **26**, 675 – 700.
- Hyndman, R. D., Yuan, T., and Moran, K., 1999, The concentration of deep sea gas hydrates from downhole electrical resistivity log sand laboratory data: *Earth and Planetary Science Letters*, **172**, 167 – 177.
- Lu, S. M., and McMechan, A. G., 2002, Estimation of gas hydrate and free gas saturation, concentration and distribution from seismic data: *Geophysics*, **67**, 582 – 593.
- Ma, Z. T., Song, H. B., and Sun, J. G., 2000, Geophysical prospecting high technologies of marine gas hydrates: *Progress in Geophysics (in Chinese)*, **15**(3), 1 – 6.
- Song, H. B., Jiang, W. W., Zhang, W. S., and Hao, T. Y., 2002, Progress on marine geophysical studies of gas hydrates: *Progress in Geophysics*, **17**(2), 224 – 229.
- Song, H. B., Song, L. X., and Jiang, W. W., 2001, Geophysical researches on marine gas hydrates

1-D Controlled source electromagnetic forward modeling

- (1): physical property: Progress in Geophysics (in Chinese), **16**(2), 118 – 126.
- Song, H. B., Zhang, L., and Jiang, W. W., 2003, Geophysical researches on marine gas hydrates (III): bottom simulating reflections: Progress in Geophysics (in Chinese), **18**(2), 182 – 187.
- Tan, H. D., Shu, Q., and Lang, J., 2004, Features of the electric field excited by electric dipole source and researches on inversion: Oil Geophysical Prospecting (in Chinese), **39**, 110 – 113.
- Yuan, J., and Edwards, R. N., 2000, The assessment of marine gas hydrate through electrical remote sounding: Hydrate without a BSR?: Geophysical

Research Letters, **27**, 2397 – 2400.

Zhao Luanxiao is a postgraduate student at Tongji University. He received a bachelor's degree in Geophysics from China University of Geoscience in 2007. His research interests are mainly seismic data processing and geophysical research on marine gas hydrate.



测到了四类波、震源点的静态模式、SV波波面尖角、反射波和透射波等。

关键词：双相各向异性，有限差分，任意偶数阶精度，数值模拟，波动方程

基于三角网格的有限差分法叠后逆时偏移 // Post-stack reverse-time migration using a finite difference method based on triangular grids, 郭书娟, 李振春, 孙小东, 叶月明, 滕厚华, 李芳, **Applied Geophysics**, 2008, 5(2), 115 - 120.

(中国石油大学(华东)地球资源与信息学院, 山东东营 257061)

摘要 与其他偏移方法相比, 逆时偏移基于精确的波动方程而不是对其近似, 用时间外推来代替深度外推。因此, 它具有良好的精度, 不受地下构造倾角和介质横向速度变化的限制。采用的三角网格差分法最大限度地保持了差分法的简单性, 同时兼有有限元法的精确性, 可直接用于起伏地表模型的正演模拟和偏移计算而无需对模型做特殊处理。本文首次尝试将三角网格差分法应用于逆时偏移中, 模型试算表明了这两种方法的结合具有较好的应用效果。

关键词: 逆时偏移; 构造倾角; 三角网格; 起伏地表

海洋天然气水合物可控源电磁法的响应特征: 一维正演模拟 // 1-D Controlled source electromagnetic forward modeling for marine gas hydrates studies, 赵峦¹, 耿建华¹, 张胜业², 杨迪琨², **Applied Geophysics**, 2008, 5(2), 121 - 126.

(1. 同济大学海洋与地球科学学院, 上海200092; 2. 中国地质大学(武汉)地球物理与空间信息学院, 武汉)

摘要: 海洋天然气水合物是一种潜在的巨大能源, 而地球物理探测技术是勘探天然气水合物资源的重要方法。本文介绍了利用可控源电磁法探测海洋天然气水合物的可行性, 在参考了大洋钻探计划(ODP)164航次对天然气水合物的采样数据的基础上建立了几种不同水合物含量的海底天然气水合物一维地电模型, 并且利用建立的模型讨论了天然气水合物的频率域电磁响应。文章就天然气水合物的电场振幅值和相位随着收发距和频率等参数的变化关系等做了相应研究, 同时就水合物厚度不同时其相应的电磁响应特征做了初

步探讨, 为海洋天然气水合物的勘探和资源评价提供了参考。

关键词: 天然气水合物, 可控源电磁法, 正演模拟, 资源评价

时频电磁技术及其在中国西部地区的应用 // The time-frequency electromagnetic method and its application effects in western China, 董卫斌, 赵晓鸣, 刘芳, 赵国, **Applied Geophysics**, 2008, 5(2), 127 - 135.

(中国石油集团东方地球物理公司, 涿州 072751)

摘要: 本文介绍了近几年来推广应用的时频电磁法技术及其在勘探逆掩构造带和深部火山岩体, 以及油气预测方面的应用效果。时频电磁技术将频率域测深与时间域测深联合在一个系统中, 可针对勘探目标的深度选择不同频率和不同类型的激发波形, 不但能提供电阻率信息, 还能提供激发极化信息, 因而在研究电性构造的同时又能检测其含油气性。时间域测深处理采用拟二维电阻率反演获得电阻率信息, 频率域测深处理引入 Cole—Cole 模型提取激发极化信息。文中以中国西部地区特殊勘探目标为实例表明, 时频电磁法在逆掩构造带勘探、深部火山岩体探测, 以及油气预测方面的有其独特的应用效果。

关键词: 时频电磁法、逆掩构造带、火山岩体、油气预测

埃及阿赫米姆古墓遗址浅层地球物理勘查 // Shallow geophysical investigations at the Akhmim archaeological site, Suhag, Egypt, Mahfooz A.Hafez^{1,3}, Magdy A.Atya¹, Azza M.Hassan¹, Motoyuki Sato², Thomas Wonik³, and Abeer A.El-Kenawy⁴, **Applied Geophysics**, 2008, 5(2), 136- 143.

(1. National Research Institute of Astronomy and Geophysics, 11722 Helwan, Cairo, Egypt; 2. Tohoku university, Center for Northeast Asian Studies, 980-8576 Sendai, Japan; 3. Leibniz Institute for Applied Geosciences (GGA), 30655 Hannover, Germany; 4. Geology Department, Faculty of Science Zagazig University., 44519 Zagazig, Egypt)

摘要: 测地雷达, 电磁勘探以及电法层析成像联合应用于古遗址的勘查, 证明是有效的方法。我们已经在阿赫米姆古墓遗址进行过地球物理测量, 测量的主要目标是确定掩埋构造以便进一步的挖掘。地球物理资料是利用GEM-300多频率电导率剖面, SIR-2000测地雷